第 29 卷第 12 期 无 机 化 学 学 报 Vol.29 No.12
2013 年 12 月 CHINESE JOURNAL OF INORGANIC CHEMISTRY 2637-2642

离子液体辅助水热法合成六方 WO_3 纳米棒束

闫智英* 李俊杰 段德良 王 伟 王家强*
(云南大学化学科学与工程学院,昆明 650091)

摘要: 提出了利用简单的离子液体 1-甲基-3-乙基-咪唑溴辅助水热法合成六方 WO_3 纳米棒束的方法,对其结构进行了表征,并讨论其形成机理。TEM 照片表明:WO_3 纳米棒束由长 200~300 nm、直径 25~30 nm 的纳米棒组装而成。离子液体 1-甲基-3-乙基-咪唑溴在纳米棒的形成过程中起到了结构导向剂的作用。

关键词: 离子液体; 纳米棒束; WO_3; 水热合成
中图分类号:0649.5 **文献标识码**:A **文章编号**: 1001-4861(2013)12-2637-06
DOI:10.3969/j.issn.1001-4861.2013.00.397

Ionic Liquid-Assisted Hydrothermal Synthesis of Hexagonal WO_3 Nanorod Bundles

YAN Zhi-Ying* LI Jun-Jie DUAN De-Liang WANG Wei WANG Jia-Qiang*
(*School of Chemical Science and Engineering, Yunnan University, Kunming* 650091, *China*)

Abstract: Hexagonal tungsten oxide (h-WO_3) was synthesized by an ionic liquid (1-methyl-3-ethyl imidazole bromide (Emim$^+$Br$^-$))-assisted hydrothermal method at 180 ℃ for 21 h. The as-synthesized products were characterized by X-ray powder diffraction (XRD), scanning electron microscopy (SEM), transmission electron microscopy (TEM), high resolution transmission electron microscopy (HRTEM) and energy dispersive X-ray spectroscopy (EDS). The results show that the morphologies of WO_3 are controlled by the amount of Emim$^+$Br$^-$. In 0.5 g Emim$^+$Br$^-$-added solution, the product is h-WO_3 nanorod bundles composed of uniform WO_3 nanorods with average diameter of 25 nm and length of 200~300 nm. The formation mechanism of h-WO_3 nanorod bundles is proposed according to the experimental results.

Key words: ionic liquid; nanorod bundle; tungsten oxide; hydrothermal synthesis

0 Introduction

One-dimensional (1-D) nanoscaled materials, such as nanotubes, nanowires, nanoribbons, nanofibers, and nanorods, have attracted intensive interest due to their novel physical properties and potential applications[1]. Among the various transition oxides, tungsten oxide has attracted great interest due to its interesting physical properties and potential applications in electrochromic or photochromic devices, secondary batteries, gas sensors and photocatalysts[2]. In particular, hexagonal form of tungsten oxide (h-WO_3) is of great interest owing to its well-known tunnel structure in which WO_6 octahedrons share their corners with each other forming hexagonal tunnels along c-axis. Hexagonal tungsten oxide has been widely investigated, especially as an intercalation host and a promising material for positive electrodes of rechargeable lithium batteries[3]. Many

收稿日期:2013-06-14。收修改稿日期:2013-09-01。
国家自然科学基金(No.21063016,No.U1033603)资助项目。
*通讯联系人。E-mail:zhyyan@ynu.edu.cn. jqwang@ynu.edu.cn

methods have been developed to synthesize h-WO_3 with 1-D nanostructures, such as thermal evaporation [4], solid-state [5], sol-gel [6] and solution-based colloidal method[7]. As a facile method, hydrothermal processes in the presence of some inorganic salts and/or surfactant have also been applied for the preparation of 1-D h-WO_3 nanostructures[8-16]. For example, Gu et al.[6,8-9] prepared h-WO_3 hierarchical structures made of nanorods/nanowires through hydrothermal process by using different sulfates (Li_2SO_4, Na_2SO_4, K_2SO_4, Rb_2SO_4) with oxalic acid as a capping agent. Tong[17] prepared h-WO_3 nanorod bundles by using pluronic P123 as surfactant with NaCl.

Recently, ILs, a kind of organic salt, have been used as media for the synthesis of inorganic nanomaterials because of the low interface tension and the associated high nucleation rate as well as high thermal stability [18-20]. While the most important advantage of IL is that IL owns highly ordered structure in the liquid system and can form hydrogen bond and electrostatic force with reaction particles, which can be used as soft-template to induce the particle to form spontaneous, well-defined, and extended ordered nanoscale materials [21-22]. Therefore, IL has received considerable attention in synthesis of the novel nano- and micro-structured inorganic materials recently. For instance, Zheng group[23] synthesized different phase and morphology TiO_2 nanoparticles via an IL-assisted method. IL not only can be used as the functional solvent but also as the template for the synthesis of inorganic materials with novel property, morphology and structure. Nowadays these advantages would encourage the ionic liquids to act as the template or capping agent in the preparation of well-defined and extended ordering of nanostructures. To the best of our knowledge, the synthesis of h-WO_3 nanorod bundles in ionic liquids has not been reported to date.

Herein, we report the preparation of h-WO_3 nanorod bundles by using a simple, inexpensive ionic liquid, 1-methyl-3-ethyl imidazole bromide ($Emim^+Br^-$) via a hydrothermal route. The effects of $Emim^+Br^-$ concentration and hydrothermal condition on the morphology were investigated, and the formation mechanism of the h-WO_3 nanorod bundles was also discussed. What differentiates our work from others is that we prepared 1-D h-WO_3 by using $Emim^+Br^-$ as a structure-directing agent without adding any other tem plates.

1 Experimental

1.1 Preparation of hexagonal tungsten oxide

All of the chemicals, such as Na_2WO_4, $Emim^+Br^-$, HCl are analytical grade and used as received without further purification. 1.63 g sodium tungstate was dissolved in 20 mL distilled water. After Na_2WO_4 solution was acidified to a pH value of 1~1.2 using 3 $mol\cdot L^{-1}$ HCl solutions, a translucent, homogeneous, and stable WO_3 sol was formed. Then 0.5 g $Emim^+Br^-$ was added to the above WO_3 sol, the solution was transferred to a 25 mL autoclave and heated at 180 ℃ for 21 h. The obtained powder was washed with water and ethanol for several times, respectively, and finally dried at 60 ℃.

1.2 Characterizations

X-ray diffraction (XRD) pattern was recorded on a Rigaku D/max-2500 X-ray diffractometer equipped with graphite monochromatized Cu$K\alpha$ radiation (with $K\alpha 2$ stripping treatment, λ =0.154 056 nm). The scanning electron microscopy (SEM) images were taken on a Hitachi S-3500N SEM. The transmission electron microscopy (TEM) images and high-resolution transmission electron microscopy (HRTEM) image were taken on a FEI TECNAI G^2 20 S-TWIN instrument performing at an accelerating voltage of 200 kV. The selected-area electron diffraction (SAED) pattern and energy-dispersive X-ray spectroscopy (EDS) were also monitored on the TEM.

2 Results and discussion

2.1 Structure and morphology of h-WO_3 nanorod bundles

The crystal structure of the synthesized tungsten oxide nanorod bundles was investigated by XRD. Fig. 1 shows that the XRD pattern of the as-synthesized nanorod bundles exhibit typical diffraction peaks of the hexagonal WO_3 (h-WO_3) with the lattice

parameters $a=b=0.729\ 8$ nm and $c=0.389\ 9$ nm (space group $P6/mmm$ (191)). All typical diffraction peaks are well indexed to the profile of hexagonal WO_3 (PDF, 33-1387). No impurity peak is observed from the XRD pattern, indicating single-phase h-WO_3. The strong and sharp diffraction peaks of the as-synthesized product also indicate the high crystallinity of the h-WO_3 nanorod bundles.

As shown in Fig.2a and 2b, large numerous, highly aligned and closely packed nanorod bundles can be observed. TEM shown in Fig.2c and 2d reveal that the WO_3 nanorod bundles are 200~300 nm in length and ~100 nm in width. In addition, a single nanorod with 25 nm in width and the stacked layers indicated with an arrow could be clearly observed from the bundles in Fig.2d, suggesting that the nanorod bundles are formed through many single rods growing together. The HRTEM image of the nanorod bundles in Fig.2e shows line defects along the length of nanorod particle

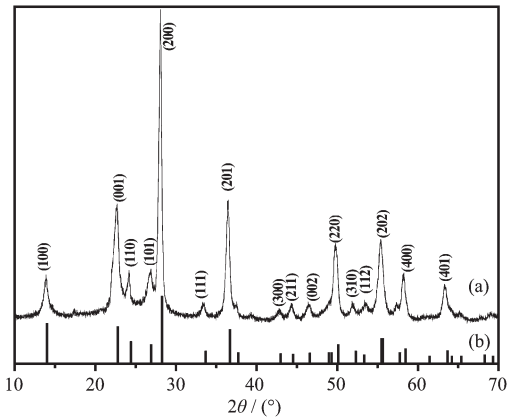

Fig.1　XRD pattern of as-synthesized h-WO_3 at 180 ℃ for 21 h (a), PDF No.33-1387(b)

(indicated with a dotted arrow) which may be due to oriented attachment of nanorods[9]. Also, The spacing of 0.382 nm between two lattice planes corresponds to the separation between (001) planes of the h-WO_3 crystal, confirming that the nanorods grow and orient longitudinally along the c-axis. This is similar to that

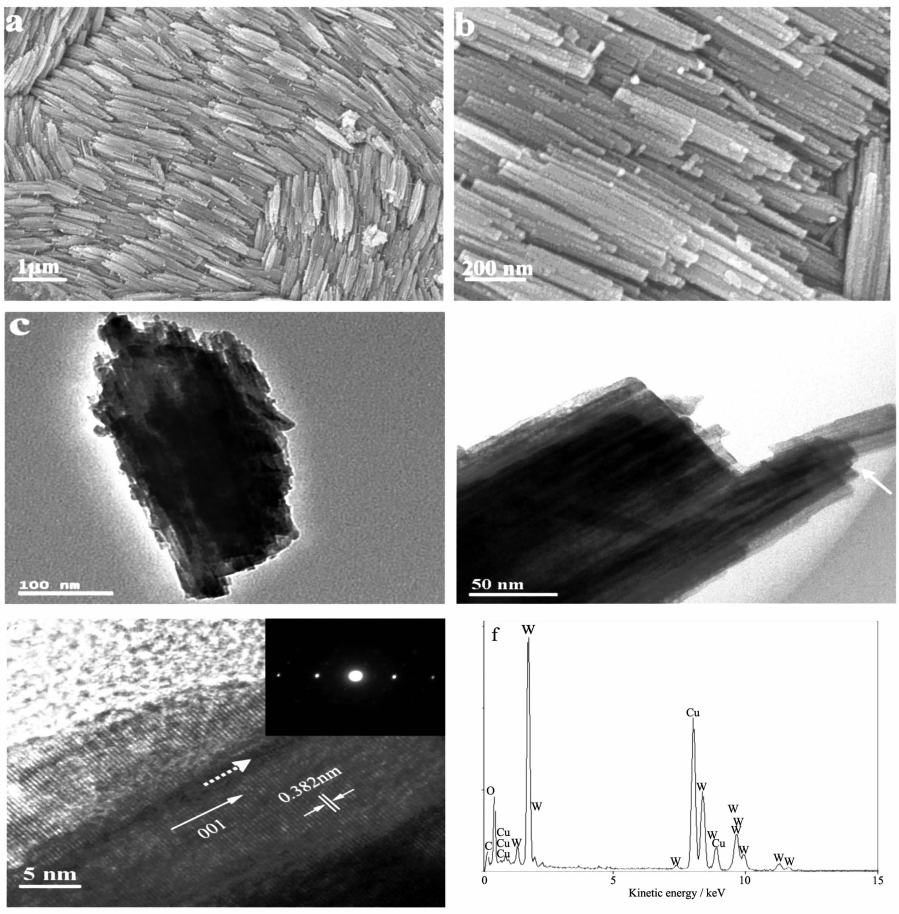

Fig.2　SEM (a) (b), TEM(c) (d), HRTEM (SAED in the inset) (e) and EDS (f) images of WO_3 nanorod bundles

obtained by using sulfates [6,8-9,15]. The corresponding SAED pattern in the inset of Fig.2e indicates the well-crystalline feature of the sample. The EDS spectrum presented in Fig.2f reveals a 3∶1 molar ratio for oxygen and tungsten elements, which solely constitute the composition of the h-WO_3.

2.2 Effect of $Emim^+Br^-$

Typical SEM images of the as-synthesized products are given in Fig.3, which clearly reveal that morphologies of as-synthesized WO_3 products in different amounts of $Emim^+Br^-$ are extremely different. As can be seen from Fig.3a, only irregular WO_3 particle can be obtained without $Emim^+Br^-$. When 0.2 g $Emim^+Br^-$ is added into the reaction systems, some individual, larger particles with diameter of 1 μm and length of 1.5~2 μm are formed as shown in Fig.3b. When the $Emim^+Br^-$ amount is 1 g, the obtained product transforms into nanorod bundles consisting of many thinner nanorods assembled together in an oriented mode (Fig.3c) as compared with the product derived from 0.5 g $Emim^+Br^-$ (Fig.2b). As a result, it may be concluded that the presence of an appropriate amount of $Emim^+Br^-$ plays a key role in the formation of the h-WO_3 nanorod bundles.

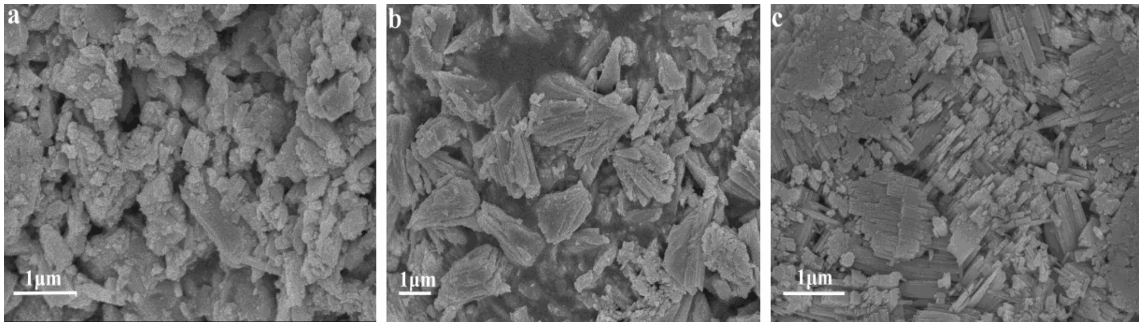

Fig.3 SEM images of WO_3 obtained by adding different amount $Emim^+Br^-$. 0 g (a), 0.2 g (b), 1 g (c)

2.3 Effect of reaction time

In order to further understand the formation of nanorod boundles, we also carried out the above-mentioned experiment in different hydrothermal times at 180 ℃ in the presence of 0.5 g $Emim^+Br^-$. As can be seen from Fig.4a, the product derived from hydrothermal treatment for 5 h is irregular particle aggregation. Upon further extending the hydrothermal time to 10 h, the product is composed of many stacked rod-shaped aggregations and some irregular

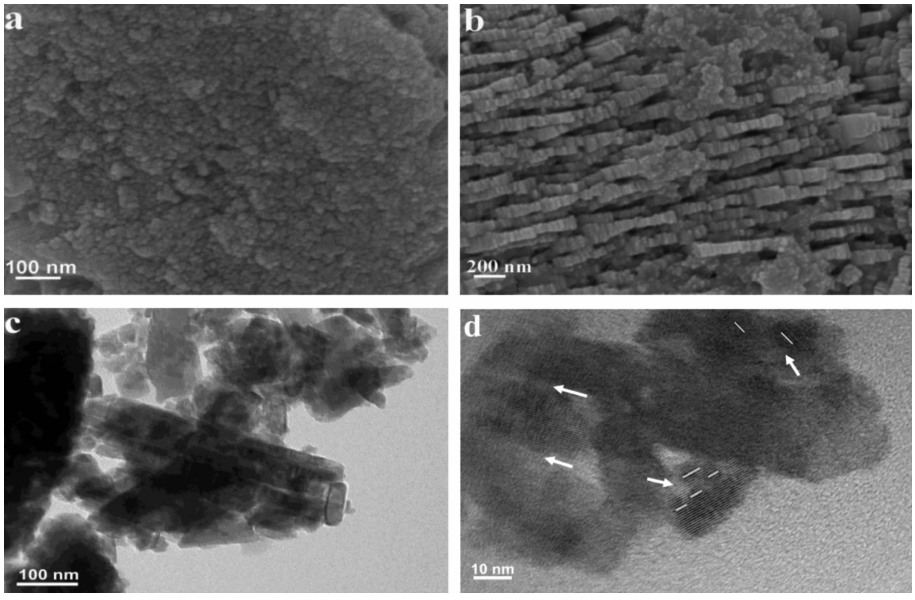

Fig.4 SEM and TEM images of WO_3 obtained at 180 ℃ with 0.5 g $Emim^+Br^-$ for different times. 5 h (a), 10 h (b)~(d)

particles (Fig.4b), implying that some WO_3 particles has transited into nanorods. Close observation reveals that stacked aggregations are actually similar to plate-like WO_3 which are formed by the oriented-attachment of single nanorod with the diameter of 25 nm and length of 300 nm as shown in Fig.4c, suggesting that under the hydrothermal conditions, the side crystal planes are able to glue together to form a larger crystal. More interestingly, the TEM image in Fig.4d further shows that nanoparticles with parallel crystallographic orientations directly combine together to form larger ones. Attached particles and the "fusion" boundaries with fuzzy crystallization are displayed clearly in the Fig.4d (indicated with arrows). The joint primary building blocks have common crystallographic orientations. This is characteristic of the oriented attachment mechanism and evidence of growth by this mechanism[24].

2.4 Mechanism of WO_3 nanorod bundles

On the basis of the above discussion, the formation mechanism for h-WO_3 nanorod bundles is proposed. Fig.5 demonstrates a schematic diagram. Generally, the presence of foreign additives can greatly influence the growth as well as morphology. This is a surface phenomenon whereby the additive molecules or ions are either physically adsorbed or chemically adsorbed on the surfaces, which can lead to anisotropic growth of nanostructures by changing the growth kinetics and surface energy of different crystal faces[25]. This concept is further explained by Gu et al.[13] that the anisotropic growth of the particles occurs by way of the specific adsorption of ions to particular crystal surface, thereby inhibiting the growth of these faces by lowering their surface energy. In the present case, we suggest that $Emim^+Br^-$ plays a role as a structure directing agent during the WO_3 nanorods growth process. In the synthesis process, large quantities of WO_3 particles may be formed by nucleation under the hydrothermal condition at the initial stages of reaction. Then WO_3 particles may orient imidazoilum ions on their surfaces by ways of imidazolium C-H $\cdots$ O_3W interactions and long-range electrostatic forces [26] or by the hydrogen bond-co-π-π stack mechanism recently proposed by Zheng et al [21,23]. Such select strong and stable surface adsorption of ions will contribute to the oriented-attachment growth of particles. Thus, WO_3 nuclei serve as seeds and grow along the c-axis direction of h-WO_3 unit cell due to the preferential absorption of $Emim^+Br^-$ on the faces parallel to the c-axis of the WO_3. Therefore, oriented growth of one-dimensional crystals appeared and nanorod-shape or plate-like products are produced. Finally, to further decrease the surface energy of the intermediates, the preformed nanoplates would continue to attach growth in an oriented fashion. Thus, the final products are formed with nanorod bundles structures.

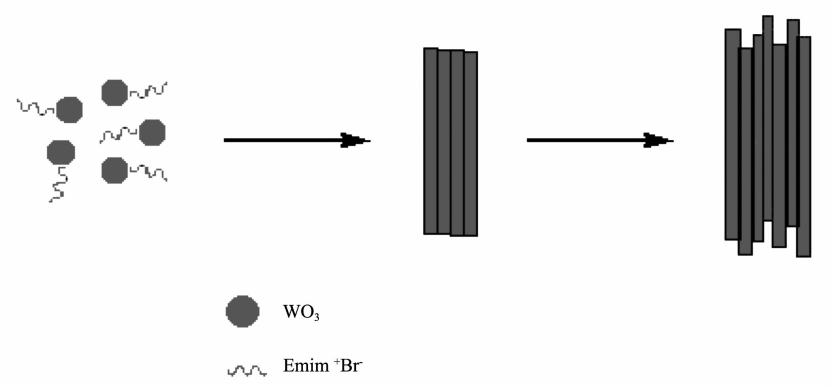

Fig.5　Formation schematic diagram of WO_3 nanorod bundles

3 Conclusions

In summary, an ionic liquid, imidazole salt (1-methyl-3-ethyl imidazole bromide, $Emim^+Br^-$)-assisted hydrothermal method is used to synthesize the hexagonal WO_3 nanorod bundles via a structure

directing growth and oriented attachment route. The obtained nanorod bundles are composed of uniform WO_3 nanorods with the average diameter of 25 nm and length of 200~300 nm.

References:

[1] Xia Y, Yang P, Sun Y, et al. *Adv. Mater.*, **2003**,**15**(5): 353-389

[2] Chen D, Ye J H. *Adv. Funct. Mater.*, **2008**,**18**:1922-1927

[3] Hibino M, Han W, Kudo T. *Solid State Ionics*, **2000**,**135**(1/3/4):61-69

[4] Wang S J, Lu W J, Cheng G, et al. *Appl. Phys. Lett.*, **2009**, **94**(26):263106-263109

[5] Wu Y, Xi Z H, Zhang G M, et al. *J. Cryst. Growth*, **2006**, **292**:143-148

[6] Gu Z J, Ma Y, Yang W S, et al. *Chem. Commun.*, **2005**,**5** (28):3597-3599

[7] CHENG Li-Fang(程利芳), ZHANG Xin-Tang(张兴堂), CHEN Yan-Hui(陈艳辉), et al. *Chinese. J. Inorg. Chem.* (*Wuji Huaxue Xuebao*), **2004**,**20**(9):1117-1122

[8] Gu Z J, Li H Q, Zhai T Y, et al. *J. Solid State Chem.*, **2007**, **180**:98-105

[9] Gu Z J, Zhai T Y, Gao B F, et al. *J. Phys. Chem. B*, **2006**, **110**:23829-23836

[10]Phuruangrat A, Ham D J, Hong S J, et al. *J. Mater. Chem.*, **2010**,**20**:1683-1690

[11]Ha J H, Muralidharan P, Kim D K. *J. Alloys Compd.*, **2009**, **475**:446-451

[12]Zhang J, Tu J P, Xia X H, et al. *J. Mater. Chem.*, **2011**,**21**: 5492-5498

[13]Peng T Y, Ke D N, Xiao J R, et al. *J. Solid State Chem.*, **2012**,**194**:250-256

[14]Lou X W, Zeng H C. *Inorg. Chem.*, **2003**,**42**(20):6169-6171

[15]Wang J M, Khoo E, Lee P S, et al. *J. Phys. Chem. C*, **2008**, **112**:14306-14312

[16]Salmaoui S, Sediri F, Gharbi N. *Polyhedron*, **2010**,**29**:1771-1775

[17]Tong P V, Hoa N D, Quang V V. *Sens. Actuators B*, **2013**, **183**:372-380

[18]Biswas K, Rao C N R. *Chem. Eur. J.*, **2007**,**13**(21):6123-6129

[19]Yang L X, Zhu Y J, Wang W W, et al. *J. Phys. Chem. B*, **2006**,**110**(13):6609-6614

[20]Shang Y, Hong J, Liu L. et al. *J. Solid State Chem.*, **2010**, **183**(3):696-701

[21]Liu X, Ma J, Zheng W. *Rev. Adv. Mater. Sci.*, **2011**,**27**:43-51

[22]Lian J B, Kim T I, Liu X D, et al. *J. Phys. Chem. C*, **2009**, **113**(21):9135-9140

[23]Zheng W J, Liu X D, Yan Z Y, et al. *ACS Nano*, **2009**,**3**(1): 115-122

[24]Zhang J, Huang F, Zhang L. *Nanoscale*, **2010**,**2**:18-34

[25]Zitoun D, Pinna N, Frolet N, et al. *J. Am. Chem. Soc.*, **2005**,**127**:15034-15035

[26]Chang H C, Jiang J C, Tsai W C, et al. *Chem. Phys. Lett.*, **2006**,**427**(4/5/6):310-316